

Printed Antifouling Electrodes for Biosensing Applications

Marc Zinggeler,* Sandra Schär, and Felix Kurth*

Cite This: *ACS Appl. Mater. Interfaces* 2022, 14, 56578–56584

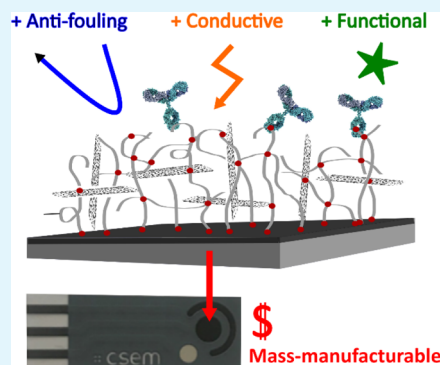
Read Online

ACCESS |

Metrics & More

Article Recommendations

ABSTRACT: Biosensors based on miniaturized, functional electrodes are of high potential for various biosensing applications, especially at the point-of-care setting among others. However, the sensor performance of such electrochemical devices is still strongly limited, especially due to surface fouling in complex sample fluids, such as blood serum. Electrode coatings based on conductive nanomaterials embedded in antifouling matrices offer a promising strategy to overcome this limitation. However, known composite coatings require long (typically >24 h) and complex fabrication processes, which pose a strong barrier for cost-effective mass manufacturing and successful commercialization. Here, we describe a novel polymer/carbon nanotube (CNT) composite coating that can be produced from an ink containing a photoreactive and antifouling copolymer as well as conductive CNTs using fast and highly scalable printing processes. Coatings were prepared on screen-printed electrodes and characterized using cyclic voltammetry (CV) and protein fouling experiments. The coatings offered an electroactive surface area (EASA) comparable to uncoated screen-printed electrodes and retained >90% of initial EASA after 1 h of exposure to concentrated bovine serum albumin solution, while uncoated electrodes decreased to <20% of initial EASA after the same treatment. Utilizing the universal crosslinking reaction of the polymer coating, antibodies against the inflammatory biomarker C-reactive protein (CRP) were photochemically immobilized on the electrodes. Functionalized electrodes were fabricated in <2 h and were successfully used to quantify nanogram-range concentrations of CRP spiked in undiluted human blood serum using a sandwich-immunoassay with electrochemical read-out, demonstrating the high potential of the platform for biosensing applications.



KEYWORDS: surface fouling, biofouling, antifouling, biosensor, point-of-care, polymer nanocomposite, carbon nanotubes (CNTs), printed electronics

INTRODUCTION

Miniaturized electrodes are of high interest for various biosensing applications. One of the most prominent commercial applications of such electrodes is electrochemical glucose meters for monitoring diabetes.¹ While glucose is measured in the low millimolar concentration range in such devices, many important biomarkers require detection concentrations of approximately 6–9 orders of magnitude lower (i.e., concentrations in the nanomolar or even picomolar range).² One of the major problems for measuring analytes in such low-concentration ranges with standard electrodes is electrode fouling, mainly due to nonspecific protein adsorption to the electrode surface upon exposure to complex body fluids, such as whole blood, blood plasma, or serum. Fouling blocks electron transfer and therefore reduces the electroactive surface area (EASA) of the sensors during read-out, causing strongly reduced sensitivity and high variability.³ To prevent these adsorption processes, surface blocking approaches, for instance, by incubation with bovine serum albumin (BSA)-containing buffers, are widely used in bioanalytical processes. However, such blocking methods, also applied for enzyme-linked immunosorbent assays (ELISAs), are not suitable to

protect electrodes due to the insulating nature of the blocking agents which, like proteins during fouling, strongly reduce the EASA of the electrodes. The same problem applies for well-known antifouling polymer coatings, such as ethylene glycol derivatives.⁴ Furthermore, extraction of proteins from the sample using semipermeable membranes, as known from small analyte (e.g., glucose) sensing,³ is not applicable as a plethora of clinically relevant biomarkers are proteins themselves.

To overcome this limitation, nanocomposite electrode coatings offer a promising strategy. In such coatings, conductive nanomaterials, for example, gold nanoparticles (AuNPs), gold nanowires (AuNWs), or CNTs, are embedded in an insulating antifouling matrix to combine the best properties of both materials: (i) high conductivity of the nanomaterial and (ii) strong antifouling properties of the

Received: September 28, 2022

Accepted: November 23, 2022

Published: December 13, 2022



matrix. However, known coatings are fabricated using long and complex processes, which pose a strong limitation for cost-effective mass manufacturing and successful commercialization. For example, early versions of nanocomposite coatings were realized using AuNP-aryl diazonium salt layers on glassy carbon electrodes, and electrochemical immunosensors that can operate in whole blood were demonstrated.^{5,6} The stepwise sensor fabrication process was very complex, involving more than six chemical surface modification steps, including at least two electrodepositions and incubation periods of several hours. Recently, a much simpler approach based on the liquid deposition of an ink containing AuNW, BSA, and glutaraldehyde (GA) crosslinker on wafer-scale gold electrodes has been developed.⁷ After crosslinking, nanocomposite layers were obtained that caused no significant EASA reduction compared to uncoated electrodes and effectively protected them from surface fouling. About 90% of initial EASA was retained even after prolonged exposure to concentrated BSA solution or undiluted human blood plasma. Electrode coatings were functionalized by antibody immobilization using carbodiimide chemistry, and the detection of the protein biomarker interleukin-6 *via* sandwich-immunoassay with electrochemical read-out was demonstrated. However, the used GA crosslinking and carbodiimide chemistry required long incubation times in a water-saturated atmosphere for 24 h and overnight, respectively. Furthermore, a quenching step is necessary to deactivate unreacted groups on the surface afterward. To reduce the cost of their system, the group replaced the expensive AuNWs with reduced graphene oxide (rGO) nanoflakes, however, still relying on the same time-consuming chemical strategy as well as employing photolithographically generated, wafer-scale gold electrodes that require heavy cleanroom infrastructure.⁸

In this work, we present a fast and highly scalable method to fabricate biochemically functional electrodes with antifouling properties. To this end, an ink consisting of a mixture of a photoreactive copolymer with strong antifouling properties and conductive CNTs was printed onto screen-printed carbon electrodes on foil, followed by drying under ambient conditions and a short UV-crosslinking step. We chose CNTs as an additive to improve the charge transfer in the functionalization layer due to their excellent electrical conductivity and commercial availability.⁹ CNTs are superior in conductivity compared to rGOs¹⁰ and cheaper than gold-based materials, for instance, AuNPs and AuNWs. The prepared electrodes were characterized by cyclic voltammetry (CV), and the composition of the nanocomposite coating was optimized to achieve both high EASA and strong antifouling properties. The EASAs of the final coatings were comparable to those of uncoated screen-printed electrodes and retained >90% of initial EASA after 1 h of exposure to the concentrated BSA solution, while uncoated electrodes dropped to <20% of their initial EASA after the same treatment due to surface fouling. Due to the universal nature of the used photocrosslinking process, biomolecules can readily be immobilized on the polymer/CNT composite layer, enabling simultaneous electrode functionalization for biosensing applications. We successfully demonstrated this process by printing a capture antibody against the inflammatory biomarker C-reactive protein (CRP) on partially crosslinked polymer/CNT coatings followed by a second drying and UV illumination step to complete the crosslinking reactions and thus to immobilize the antibody. The hereby prepared biosensing electrodes enabled

quantifying CRP in spiked undiluted human blood plasma using a sandwich-immunoassay with electrochemical read-out.

MATERIALS AND METHODS

Screen-Printed Electrodes. Screen-printed electrodes were produced at CSEM using a screen-printing sheet-to-sheet process previously described.¹¹ The described printing process was conducted with a screen printer from Aurel (Aurel S.P.A., VS1520A), and the applied Ag/AgCl ink weight ratio was 60/40. Similar electrodes are also commercially available from different companies, such as Metrohm (DropSens 11L, C11L), PalmSens (CSCL4W), or Zimmerpeacock (A-AC-CC-101-N) among others.

EASA Measurements. Electrodes were connected to a potentiostat (PalmSens, MultiTrace 4.3) and immersed in 10 mM potassium hexacyanoferrate(III) (Sigma-Aldrich, 244023) in phosphate-buffered saline (PBS) (Sigma-Aldrich, P4417). Three CV scans with different scan rates (30, 50, 70, and 90 mV/s) were measured from 1 to -1 V against the printed Ag/AgCl reference electrode (RE), and the third scan was used for analysis. The peak reduction currents were extracted by the potentiostat software (PSTrace 5.7) and plotted against the square root of the scan rate. The slope of the best linear fit was subsequently chosen for EASA calculation using the Randles-Sevcik equation¹²

$$i_p = \left\{ 0.4463nFAC \left(\frac{nFD}{RT} \right)^{0.5} \right\} \cdot \nu^{0.5}$$

where i_p is the peak reduction current, n is the number of electrons transferred in the redox reaction ($= 1$ for ferricyanide), F is Faraday's constant ($= 96485.3$ C/mol), A is the EASA, C is the concentration of the ferricyanide ($= 10$ mM), D is the diffusion coefficient of ferricyanide ($= 7.26 \times 10^{-6}$ cm² s⁻¹), R is the universal gas constant ($= 8.314$ J K⁻¹ mol⁻¹), T is the temperature of the solution, and ν is the scan rate. The term in the curly brackets corresponds to the slope of the linear fit and was used for EASA calculation by resolving the term to A .

Surface Fouling Measurements. EASA measurements were performed before and after immersing the electrodes in 40 mg/mL BSA (Sigma-Aldrich, A2153) in PBS (pH 7.4) for defined periods at room temperature. After immersion in the protein solution, the electrodes were rinsed with deionized water prior to measurement.

Preparation of Polymer/CNT Coatings. The photoreactive copolymer poly(*N,N*-dimethylacrylamide-*stat*-methacryloyloxy-benzophenone) was kindly provided by the Laboratory for Chemistry and Physics of Interfaces, Department for Microsystems Engineering at the University of Freiburg, Germany. It was synthesized by standard free-radical polymerization of *N,N*-dimethylacrylamide (95 mol %) and methacryloyloxybenzophenone (5 mol-%) as described elsewhere and was obtained as a white powder with a yield of about 50% and a molecular weight of about 750 000 g/mol.¹³ Multiwalled CNTs, produced *via* the catalytic chemical vapor deposition process and -COOH surface modified, were obtained commercially (Nanocyl, 3101). "Polymer-only" formulations were prepared by dissolving the polymer at different concentrations (0.46–9.12 mg/mL) in ethanol. "Polymer/CNT" formulations were prepared by mixing the polymer and CNT solutions, both 9.12 mg/mL in ethanol, at different ratios (2.5/1–10/1). CNTs were dispersed by sonication for 45 min. 0.5 μ L of the solution was deposited onto the working electrode (WE) using a pipette followed by drying at ambient conditions for 5 min. Coatings were crosslinked by 434 s UV illumination (2.3 mW/cm², 254 nm, 1 J/cm²).

SEM Analysis. Blank/coated electrodes were sputter-coated with a thin gold layer (10 nm) by cathode sputtering (Balzers SCD 030 Au coater + Balzers QSG 301). Imaging was carried out by the detection of secondary electrons using an in-lens detector at an accelerating voltage of 20 kV (S-4100 Scanning Electron Microscope, Hitachi S 4100 SEM).

Electrode Functionalization and CRP Biosensing. Polymer/CNT formulation with a ratio of 2.5/1 was prepared as described

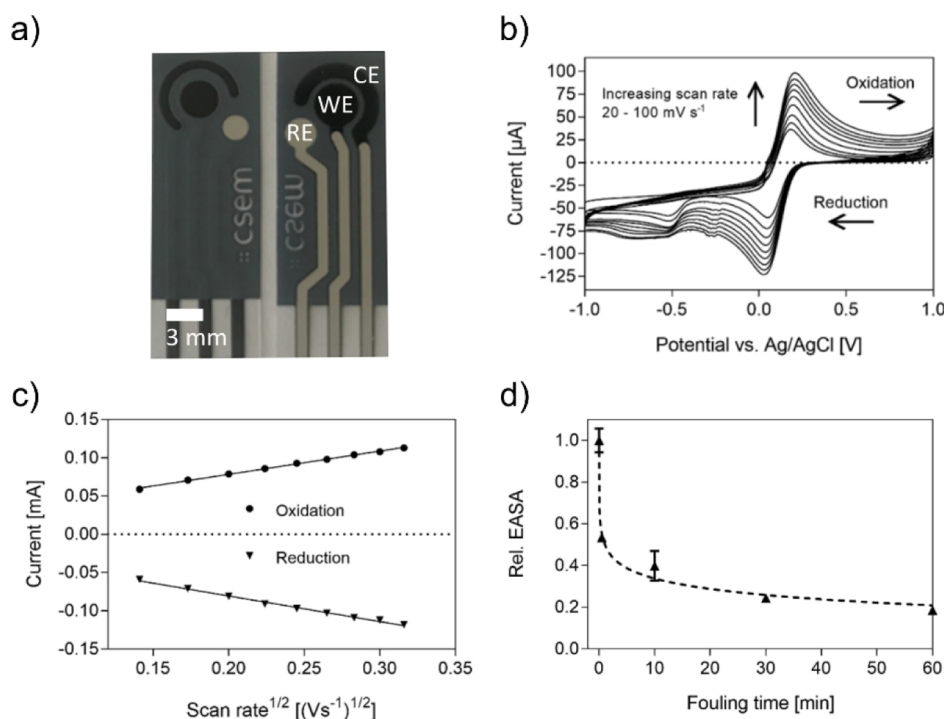


Figure 1. Electrochemical setup and measurements to determine the EASA and surface fouling of electrodes. (A) Image of screen-printed, miniaturized three-electrode setup on foil (left: front side, right: back side) with RE, WE, and CE. (B) CV scans were measured in a ferricyanide solution with different scan rates. (C) Plotted peak currents for oxidation/reduction vs. the square root of the scan rate including linear fits. The correlation coefficients are R^2 (oxidation) = 0.9977 and R^2 (reduction) = 0.9936. (D) Surface fouling curve measured for uncoated WE in the BSA solution (40 mg/mL). After each incubation period, the EASA was determined from the slope of the linear fit curve of the reduction currents as shown in (C). Values were normalized to the EASA of an electrode not exposed to BSA (equals fouling time of 0 min). Mean values and standard deviations are shown for $n = 3$.

above. 0.5 μL of the solution was deposited onto the WE using a pipette followed by drying at ambient conditions for 5 min. Coating was partially crosslinked by UV illumination (17 mW/cm^2 , 365 nm, 1 J/cm^2) for 59 s. 5 μL of 10 $\mu\text{g}/\text{mL}$ CRP capture antibody (R&D Systems, MAB17071-500) in PBS was pipetted onto WE followed by drying at ambient conditions for 1 h. Antibody immobilization and crosslinking were completed by 434 s UV illumination (2.3 mW/cm^2 , 254 nm, 1 J/cm^2). Electrodes were immersed in assay buffer (PBS, 1% BSA, 0.1% Tween 20) for 10 min for washing. Sandwich-immunoassay was performed by stepwise incubation: (1) 10 min with CRP (R&D Systems, 1707-CR-200)-spiked serum (BBI Solutions, CRP-depleted serum, SF100-2), (2) 5 min with 1 $\mu\text{g}/\text{mL}$ biotinylated CRP detection antibody (R&D Systems, BAM17072) in assay buffer, (3) 10 min with 1:50 diluted streptavidin-HRP in assay buffer, and (4) 10 min with TMB/ H_2O_2 solution (Sigma-Aldrich, T8665). The electrodes were washed with an assay buffer between the incubation steps. During the last incubation step (i.e., in TMB/ H_2O_2), the electrodes were connected to a potentiostat (PalmSens, MultiTrace 4.3), and after 10 min, incubation was completed. Chronoamperometry was measured at an applied potential of 0 V against the printed Ag/AgCl RE for 60 s. Data was analyzed using the potentiostat software (PSTrace 5.7), Microsoft Excel, and GraphPad Prism 9. Data fitting was conducted in GraphPad Prism using a nonlinear sigmoidal regression model with the Hill coefficient defined as 1. The limit of detection (LOD) current was calculated by $\text{LOD signal} = \text{average current of blanks} + 3 \text{ times standard deviation of blanks}$, and the limit of quantification (LOQ) current was calculated by $\text{LOQ signal} = \text{average current of blanks} + 10 \text{ times standard deviation of blanks}$. LOD and LOQ concentrations were interpolated using the nonlinear sigmoidal regression model.

RESULTS AND DISCUSSION

Electrode Fabrication and Characterization. To set the stage for a low-cost, point-of-care (POC) approach, electrodes were printed on foil by a layer-by-layer screen-printing process. While the electrodes were printed at approximately A4 scale using sheet-to-sheet processes, similar electrodes are fabricated at an industrial scale using roll-to-roll processes and are commercially available, which underlines the compatibility of our approach with established manufacturing routes. A miniaturized three-electrode system was selected as a basis for the study to allow for voltammetric and amperometric measurements (Figure 1a). The electrode system consists of a carbon working electrode (WE) and a carbon counter electrode (CE) as well as a Ag/AgCl pseudo reference electrode (RE) that offers a stable potential in solutions with constant chloride concentration. The electrodes are separated from each other by a dielectric insulation layer. To determine the EASA of the WE and its susceptibility for surface fouling, a CV method was selected.⁷ Hereby, CV scans with different scan rates were performed in a ferricyanide solution with a defined concentration and diffusion coefficient. From these measurements, oxidation and reduction peak currents (Figure 1b) were plotted as a function of the square root of the scan rate (Figure 1c), and the EASA of the electrode was then calculated from the slope of the linear fit curve using the Randles–Ševčík equation.¹² Using this method, an EASA of 4.5 mm^2 was determined for uncoated WE with a 3 mm diameter. This corresponds to about 64% of the geometrical surface area and is comparable to values reported in the literature for screen-printed carbon electrodes.¹⁴ A value

smaller than 100% is characteristic of these electrodes due to insulating binder materials used as additives in screen-printing pastes. Furthermore, it is to be noted that the absolute EASA values determined using the CV method might be subject to uncertainty caused by, for instance, the used redox species.¹⁵ However, relative values are of importance for this work, and all measured EASA values for both blank and coated electrodes exposed to protein-containing solutions are therefore normalized to the value determined for blank electrodes measured in a protein-free buffer solution.

To assess the susceptibility of electrodes to surface fouling due to protein adsorption, the EASAs of electrodes were determined before and after immersion in solutions containing 40 mg/mL BSA, which corresponds to the approximate physiological albumin concentration in human blood.² The results of a fouling study using uncoated electrodes are shown in Figure 1d. Uncoated electrodes lost almost 50% of EASA upon mere contact with the solution and decreased by more than 80% of the initial EASA after an exposure of 1 h only. Notably, the CV measurement results were recorded after rinsing the electrodes thoroughly with deionized water, which indicates strong, possibly partially irreversible protein adsorption.

Photoreactive copolymers offer a versatile tool to protect surfaces from protein adsorption by forming crosslinked hydrogel thin films.¹³ We deposited different amounts of polydimethyl acrylamide with 5% benzophenone photocrosslinker by drop casting from ethanolic solutions onto the WEs followed by UV crosslinking. Deposition of increasing polymer amounts led to decreasing electrode surface fouling, which can be explained by a gradual generation of a closed protective coating upon ink drying and crosslinking on the rough electrode surface (Figure 2a). When depositing at least 2.28 μg of polymer/WE, no initial decrease in EASA over time could be observed anymore, suggesting negligible to no remaining fouling effects on the electrodes. The deposited polymer amount of 2.28 $\mu\text{g}/\text{WE}$ hereby corresponds to a calculated dry polymer layer thickness in the range of 300 nm, assuming a polymer density of 1 g/mL. To also allow for POC protein assays longer than a few minutes, we chose a fixed polymer load of 4.56 $\mu\text{g}/\text{mL}$ in all the following experiments as this amount stabilized the EASA well over the recorded period (cf. Figure 2a, right).

While polymer coating led to fouling-resistant electrodes, it simultaneously caused a strong reduction in EASA of up to 70% compared to uncoated electrodes measured in buffer solution (Figure 2b) due to the insulating nature of the polymer, which blocks charge transfer and serves as a diffusion barrier for redox species. To compensate for this loss in charge transfer, increasing amounts of conductive CNTs were incorporated into the polymer layers by mixing them directly into the polymer ink before deposition. With an optimum polymer/CNT weight ratio of 2.5/1, stable and strongly fouling-resistant electrodes with an EASA comparable to untreated, blank electrodes were achieved (Figure 2b). While coatings with a polymer/CNT ratio higher than 2.5/1 (i.e., lower CNT load) lead to decreased EASA values (Figure 2b), solubility problems and instable coating layers were observed for polymer/CNT ratios lower than 2.5/1 (i.e., higher CNT load; data not shown). Qualitative SEM analyses of the coated electrodes show that the typical screen-printed carbon flakes are densely covered by a polymer/CNT “web” (Figure 3). Additional in-depth analysis of the surface morphological

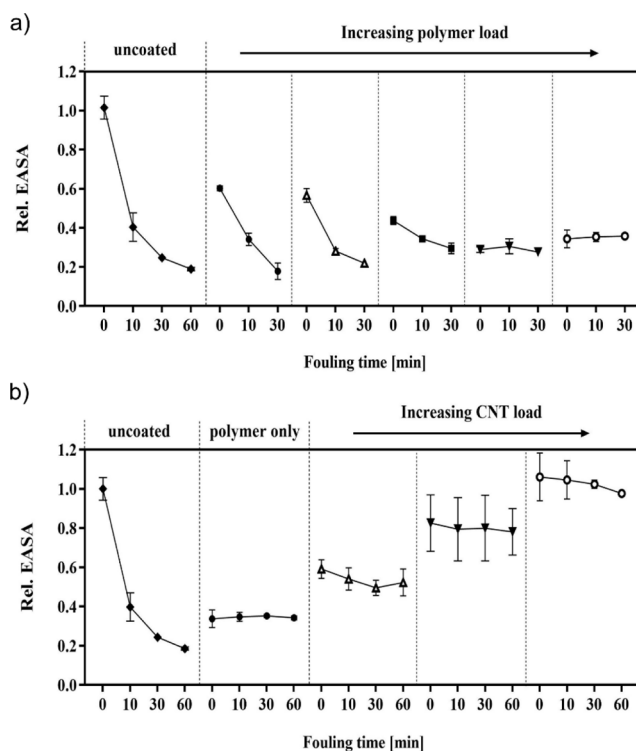


Figure 2. Generated results during antifouling coating development. (A) Measured fouling curves for uncoated and polymer-coated electrodes. Polymer loads in microgram/WE from left to right: 0.23, 0.46, 1.14, 2.28, and 4.56. (B) Measured fouling curves for uncoated and coated electrodes with different coating compositions. The deposited polymer amount was 4.56 $\mu\text{g}/\text{WE}$ for all coatings. While the “polymer-only” coating contained no added CNTs, increasing CNT amounts were added to the composite coatings. Polymer/CNT weight ratio from left to right: 10/1, 4/1, and 2.5/1. Mean values and standard deviations are shown in both plots for $n = 3$.

changes due to varying CNT loads will help better understand the correlation of surface morphology toward EASA (not part of this study).

Electrochemical Protein Biosensing. Due to the universal nature of the photocrosslinking chemistry of the deposited polymer coatings (i.e., C, H insertion reactions),¹⁶ biomolecules and other functional organic molecules containing available C–H groups can be covalently immobilized to the polymer layers. This fast and highly efficient functionalization chemistry has previously been used for the realization of optical protein biosensors^{17–20} and was used in this work for electrode functionalization and the realization of an electrochemical protein biosensor. To this end, the deposited polymer/CNT electrode coatings were only partially crosslinked during the first UV exposure. Subsequently, a capture antibody against CRP, which was selected as a model protein biomarker for this study, was deposited by drop casting the antibody solution onto the coated WE. After drying, a second UV illumination was performed to photochemically immobilize the antibody and complete the crosslinking reactions in the polymer/CNT film. Although the biomolecule could in principle be added to the initial polymer/CNT mixture, which would reduce the functionalization process to a single liquid deposition step, the two-step process was selected to enable the use of different coating solution formulations—that is to say—solvent-based (here: ethanol) and water-based formulations. Whereby the solvent-based solution is required

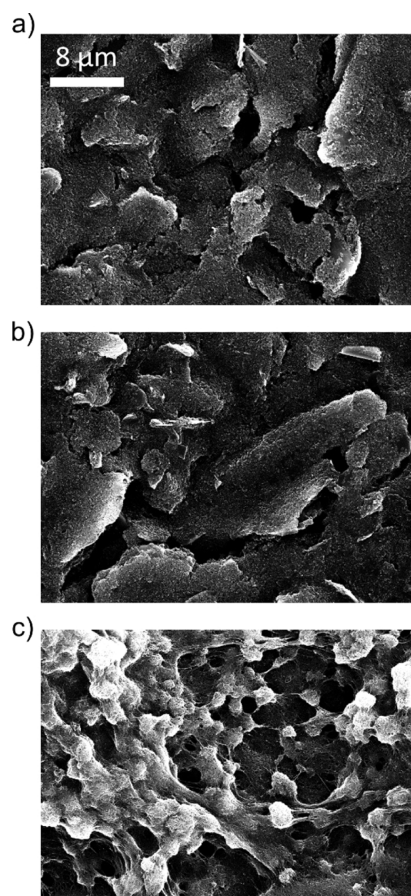


Figure 3. SEM micrographs of blank (a), polymer-coated ($4.56 \mu\text{g}/\text{WE}$) (b), and polymer/CNT-coated ($4.56 \mu\text{g}$ polymer/WE and polymer/CNT weight ratio of 2.5/1) electrodes (c). The shared scale bar is depicted in the top image.

to dissolve the polymer and the sonication is essential for dispersion of the CNTs in solution, both solvent and sonication cause biomolecule denaturation. Another advantage of the two-step process is that the desired antibody can be immobilized from a fresh stock solution prior to the use of the platform offering high experimental flexibility. Nevertheless, the complete fabrication process to obtain biochemically functional electrodes with antifouling properties took <2 h, which is more than 10-fold faster than previously reported preparation methods.^{7,8} The functionalized electrodes were then used for the detection of CRP in spiked undiluted human blood serum by a sandwich-immunoassay with electrochemical read-out (Figure 4).

For the CRP assay, the electrodes were stepwise incubated in (1) CRP-spiked serum samples (10 min), (2) biotinylated CRP detection antibody (5 min), (3) streptavidin-horseradish peroxidase (HRP; 10 min), and (4) TMB/ H_2O_2 solution (10 min). The electrodes were washed with buffer between each incubation step. In this fast assay, the obtained concentration of HRP bound to the electrode surface is determined by the CRP concentration in the samples and ultimately oxidizes TMB with a defined activity. The concentration of oxidized TMB can then be correlated to the CRP concentration, which is typically done optically using commercial ELISA platforms due to the blue color of the oxidized TMB (turning yellow when treated with acid). However, the oxidized TMB can also be measured electrochemically. In our miniaturized three-

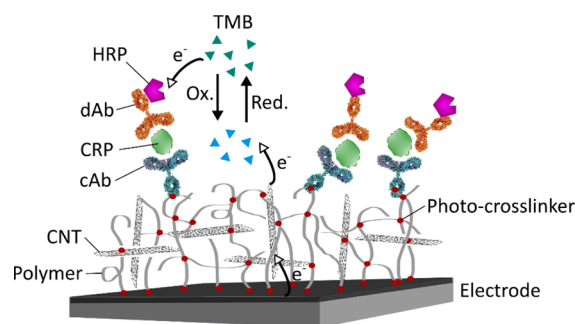


Figure 4. Schematic illustration of the functionalized composite electrodes and the employed sandwich-immunoassay strategy to generate an electrochemically measurable signal. cAb: capture antibody, dAb: detection antibody, CRP: C-reactive protein, HRP: horseradish peroxidase, TMB: 3,3',5,5'-tetramethylbenzidine.

electrode sensor system, this was performed by chronoamperometric reduction of the oxidized TMB. Hereby, the WE was fixed to a potential of 0 V versus the printed Ag/AgCl RE, and the current was measured between the WE and the CE for 1 min (Figure 5a).

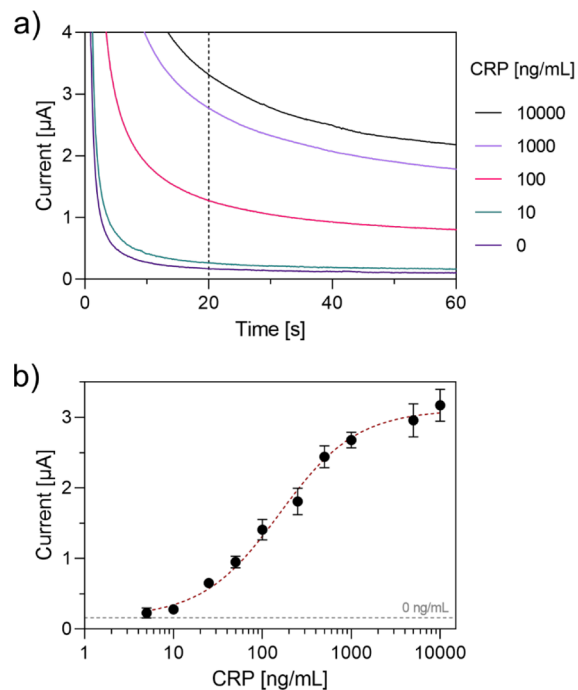


Figure 5. Results of the realized CRP biosensor platform. (A) Measured reduction currents during read-out for different exemplary CRP concentrations in undiluted human blood serum. (B) Calibration curve obtained by plotting the measured reduction currents after 20 s vs. CRP concentration. Mean values and standard deviations are shown ($n = 3$). The red dashed line shows the best fit using a nonlinear sigmoidal model. The gray dashed line depicts the current value at 0 ng/mL CRP in undiluted serum.

To characterize the LOD and LOQ as well as the concentration range, the developed electrochemical platform was used to measure increasing CRP concentrations spiked to undiluted human blood serum following the protocol detailed above. We obtained a CRP calibration curve that plots the measured currents after 20 s of electrochemical recording as a function of the CRP concentration (Figure 5b). The data

points were extracted after 20 s of electrochemical recording because data obtained at this time offers a good compromise between the high signal that decreases over time and low variability, the latter of which is high at early time scales due to, for instance, capacitive charging effects of the electrodes. The biosensor demonstrator was capable of quantifying CRP in undiluted human serum over the complete nanogram/milliliter range, which is relevant for a plethora of protein biomarkers. The calculated LOD is 3.1 ng/mL, and the calculated LOQ is 11.9 ng/mL. Although the very high sensitivity for CRP is below clinically relevant concentration ranges that are considered in the microgram/milliliter range in human blood for a variety of health complications, such as cardiovascular disease and numerous other clinical conditions (healthy: <1 $\mu\text{g/mL}$, medium risk: 1–3 $\mu\text{g/mL}$, high risk: >3 $\mu\text{g/mL}$, and acute infections: >100 $\mu\text{g/mL}$),^{21–23} the developed high-sensitivity assay, on the one hand, quantifies CRP in concentration ranges as, for instance, commercially available ELISA kits as well as other reported POC systems.^{24–26} On the other hand, the high sensitivity proves its potential for low-concentration protein biomarker quantification in solutions with heavy protein background as well as strong sensor fouling in general. Moreover, since samples with comparably high CRP concentrations can easily be diluted to a targeted, suitable measurement range, the described sensor represents a valid POC sensor solution for CRP quantification in serum.

CONCLUSIONS

Polymer–CNT composite layers combine strong antifouling properties and high conductivity for electrical sensor systems. In this study, we show that printing a mixture of photoreactive copolymer and CNTs offers a very fast and cost-effective method of fabricating antifouling electrochemical sensor systems. The simultaneously protective as well as conductive prepared films can readily be functionalized with biomolecules rendering the sensors ideally suited for various biosensing applications in clinical samples with a generally high protein load. While similar existing nanocomposite coatings require >24 h of preparation, our described functional “biosensing ready” coatings can be produced with the presented method in <2 h, even in a nonproduction research environment with less process automation. The fabrication process that solely relies on liquid deposition, drying, and UV illumination steps has a high potential for mass manufacturing of functional, antifouling sensing electrodes for integration into cost-effective POC devices. As an alternative to the here applied drop-casting process, inkjet printing holds strong potential for the mass fabrication of the presented sensors. Due to its process technology, which is a noncontact printing method ejecting picoliter droplets with a high printing resolution, the fabrication route could benefit in terms of further miniaturization and less material waste.²⁷ Future research is intended to focus on long-term (days) characterization of the protective properties to identify its adaptability for continuous monitoring applications as well as introducing other protein biomarker systems to widen the scope of clinical applicability. Next to biomarker detection in blood, the use of the presented sensor system for other body fluids is of interest.

AUTHOR INFORMATION

Corresponding Authors

Marc Zinggeler – Centre Suisse d'électronique et de Microtechnique SA (CSEM), Muttenz 4132, Switzerland;

Present Address: Tecan Schweiz AG, Seestrasse 103, 8708 Männedorf, Switzerland; Phone: +41 (44) 922 8115; Email: marc.zinggeler@tecan.com

Felix Kurth – Centre Suisse d'électronique et de Microtechnique SA (CSEM), Muttenz 4132, Switzerland; Present Address: Centre suisse d'électronique et de microtechnique SA (CSEM), Switzerland Innovation Park Main Campus, Hegenheimerweg 167 A, 4123 Allschwil, Switzerland; orcid.org/0000-0002-3211-6820; Phone: +41 61 690 6018; Email: felix.kurth@csem.ch

Author

Sandra Schär – Centre Suisse d'électronique et de Microtechnique SA (CSEM), Muttenz 4132, Switzerland

Complete contact information is available at:

<https://pubs.acs.org/10.1021/acsami.2c17557>

Author Contributions

M.Z. planned the study and acquired funding. M.Z. and S.S. designed experiments. S.S. performed experiments and data analysis. M.Z. and F.K. defined the scope of the manuscript. M.Z., S.S., and F.K. cowrote the manuscript. All authors have given approval to the final version of the manuscript.

Funding

The research was funded by the Swiss Nanoscience Institute (SNI) of the University of Basel under the project acronym “PEPS”.

Notes

The authors declare no competing financial interest.

ACKNOWLEDGMENTS

The authors thank Prof. Dr. Jürgen Rühle and Dr. Thomas Brandstetter from the University of Freiburg, Germany for the polymer supply. Nicolas Glaser and Christian Seitz are thanked for screen-printed electrodes. The authors furthermore thank the PEPS project consortium for fruitful discussions and the SNI for research funding.

REFERENCES

- (1) Heller, A.; Feldman, B. Electrochemistry in Diabetes Management. *Acc. Chem. Res.* **2010**, *43*, 963–973.
- (2) Anderson, N. L.; Anderson, N. G. The Human Plasma Proteome. *Mol. Cell. Proteomics* **2002**, *1*, 845–867.
- (3) Barfidokht, A.; Gooding, J. J. Approaches Toward Allowing Electroanalytical Devices to Be Used in Biological Fluids. *Electroanalysis* **2014**, *26*, 1182–1196.
- (4) Hui, N.; Sun, X.; Niu, S.; Luo, X. PEGylated Polyaniline Nanofibers: Antifouling and Conducting Biomaterial for Electrochemical DNA Sensing. *ACS Appl. Mater. Interfaces* **2017**, *9*, 2914–2923.
- (5) Liu, G.; Iyengar, S. G.; Gooding, J. J. An Electrochemical Impedance Immunosensor Based on Gold Nanoparticle-Modified Electrodes for the Detection of HbA1c in Human Blood. *Electroanalysis* **2012**, *24*, 1509–1516.
- (6) Liu, G.; Iyengar, S. G.; Gooding, J. J. An Amperometric Immunosensor Based on a Gold Nanoparticle-Diazonium Salt Modified Sensing Interface for the Detection of HbA1c in Human Blood. *Electroanalysis* **2013**, *25*, 881–887.
- (7) Sabaté del Río, J.; Henry, O. Y. F.; Jolly, P.; Ingber, D. E. An Antifouling Coating That Enables Affinity-Based Electrochemical Biosensing in Complex Biological Fluids. *Nat. Nanotechnol.* **2019**, *14*, 1143–1149.

- (8) Zupančič, U.; Jolly, P.; Estrela, P.; Moschou, D.; Ingber, D. E. Graphene Enabled Low-Noise Surface Chemistry for Multiplexed Sepsis Biomarker Detection in Whole Blood. *Adv. Funct. Mater.* **2021**, *31*, 2010638.
- (9) Choudhary, M.; Sharma, A.; Aravind Raj, S. A.; Sultan, M. T. H.; Hui, D.; Shah, A. U. Contemporary Review on Carbon Nanotube (CNT) Composites and Their Impact on Multifarious Applications. *Nanotechnol. Rev.* **2022**, *11*, 2632–2660.
- (10) Kong, L.; Yin, X.; Xu, H.; Yuan, X.; Wang, T.; Xu, Z.; Huang, J.; Yang, R.; Fan, H. Powerful Absorbing and Lightweight Electromagnetic Shielding CNTs/RGO Composite. *Carbon* **2019**, *145*, 61–66.
- (11) Tang, Y.; Petropoulos, K.; Kurth, F.; Gao, H.; Migliorelli, D.; Guenat, O.; Generelli, S. Screen-Printed Glucose Sensors Modified with Cellulose Nanocrystals (CNCs) for Cell Culture Monitoring. *Biosensors* **2020**, *10*, 125.
- (12) Elgrishi, N.; Rountree, K. J.; McCarthy, B. D.; Rountree, E. S.; Eisenhart, T. T.; Dempsey, J. L. A Practical Beginner's Guide to Cyclic Voltammetry. *J. Chem. Educ.* **2018**, *95*, 197–206.
- (13) Wörz, A.; Berchtold, B.; Moosmann, K.; Prucker, O.; Rühle, J. Protein-Resistant Polymer Surfaces. *J. Mater. Chem.* **2012**, *22*, 19547–19561.
- (14) Bollella, P.; Fusco, G.; Stevar, D.; Gorton, L.; Ludwig, R.; Ma, S.; Boer, H.; Koivula, A.; Tortolini, C.; Favero, G.; Antiochia, R.; Mazzei, F. A Glucose/Oxygen Enzymatic Fuel Cell Based on Gold Nanoparticles Modified Graphene Screen-Printed Electrode. Proof-of-Concept in Human Saliva. *Sens. Actuators, B* **2018**, *256*, 921–930.
- (15) García-Miranda Ferrari, A. G. M.; Foster, C. W.; Kelly, P. J.; Brownson, D. A. C.; Banks, C. E. Determination of the Electrochemical Area of Screen-Printed Electrochemical Sensing Platforms. *Biosensors* **2018**, *8*, 53.
- (16) Prucker, O.; Brandstetter, T.; Rühle, J. Surface-Attached Hydrogel Coatings via C,H-Insertion Crosslinking for Biomedical and Bioanalytical Applications (Review). *Biointerphases* **2018**, *13*, 010801.
- (17) Zinggeler, M.; Schönberg, J. N.; Fosso, P. L.; Brandstetter, T.; Rühle, J. Functional Cryogel Microstructures Prepared by Light-Induced Cross-Linking of a Photoreactive Copolymer. *ACS Appl. Mater. Interfaces* **2017**, *9*, 12165–12170.
- (18) Zinggeler, M.; Fosso, P. L.; Hao, Y.; Brandstetter, T.; Rühle, J. Preparation of Linear Cryogel Arrays as a Microfluidic Platform for Immunochromatographic Assays. *Anal. Chem.* **2017**, *89*, 5697–5701.
- (19) Scherag, F. D.; Mader, A.; Zinggeler, M.; Birsner, N.; Kneusel, R. E.; Brandstetter, T.; Rühle, J. Blocking-Free and Substrate-Independent Serological Microarray Immunoassays. *Biomacromolecules* **2018**, *19*, 4641–4649.
- (20) Fosso Tene, P. L.; Stumpf, A.; Zinggeler, M.; Reuck, V.; Malik, A.; Weigel, W.; Müller, M.; Kneusel, R.; Brandstetter, T.; Rühle, J. Linear Cryogel Arrays: On the Fast Track for Borreliosis Detection. *Anal. Chem.* **2021**, *93*, 12426–12433.
- (21) Young, B.; Gleeson, M.; Cripps, A. W. C-Reactive Protein: A Critical Review. *Pathology* **1991**, *23*, 118–124.
- (22) Serbéé, M. J. V.; Dulfer, E. A.; Dirks, K. K. T.; Bosboom, R.; Robberts, B.; Wertheim, H. F. L.; Mulder, B.; de Jonge, M. I.; Schaars, C. F.; Swanink, C. M. A.; Cremers, A. J. H. C-Reactive Protein to Rule out Complicated Pneumococcal Disease Manifestations: A Retrospective Cohort Study in Adults with Pneumococcal Bacteraemia. *Int. J. Infect. Dis.* **2021**, *111*, 172–178.
- (23) Castro, A. R.; Silva, S. O.; Soares, S. C. The Use of High Sensitivity C-Reactive Protein in Cardiovascular Disease Detection. *J. Pharm. Pharm. Sci.* **2018**, *21*, 496–503.
- (24) Oh, Y. K.; Joung, H. A.; Kim, S.; Kim, M. G. Vertical Flow Immunoassay (VFA) Biosensor for a Rapid One-Step Immunoassay. *Lab Chip* **2013**, *13*, 768–772.
- (25) Dong, M.; Wu, J.; Ma, Z.; Peretz-Soroka, H.; Zhang, M.; Komenda, P.; Tangri, N.; Liu, Y.; Rigatto, C.; Lin, F. Rapid and Low-Cost CRP Measurement by Integrating a Paper-Based Microfluidic Immunoassay with Smartphone (CRP-Chip). *Sensors* **2017**, *17*, 684.
- (26) Meyer, M. H. F.; Hartmann, M.; Krause, H. J.; Blankenstein, G.; Mueller-Chorus, B.; Oster, J.; Mieth, P.; Keusgen, M. CRP Determination Based on a Novel Magnetic Biosensor. *Biosens. Bioelectron.* **2007**, *22*, 973–979.
- (27) Singh, M.; Haverinen, H. M.; Dhagat, P.; Jabbour, G. E. Inkjet Printing-Process and Its Applications. *Adv. Mater.* **2010**, *22*, 673–685.

Recommended by ACS

Structural Remodeling Mechanism of the Toxic Amyloid Fibrillary Mediated by Epigallocatechin-3-gallate

Nan Zhang, Yuan Cheng, *et al.*

DECEMBER 13, 2022
ACS OMEGA

READ 

Simple Multifunctional PTX@Ce6 Nanomedicine for Eradicating Tumor in the Combination of Photodynamic Therapy and Metronomic Chemotherapy

Mengxuan Li, Juan Li, *et al.*

DECEMBER 15, 2022
ACS OMEGA

READ 

Green Synthesis, Surface Activity, Micellar Aggregation, and Foam Properties of Amide Quaternary Ammonium Surfactants

Xinru Jia, Bao-Cai Xu, *et al.*

DECEMBER 15, 2022
ACS OMEGA

READ 

Enhanced Ionic Current Rectification through Innovative Integration of Polyelectrolyte Bilayers and Charged-Wall Smart Nanochannels

Hossein Dartoomi, Seyed Nezameddin Ashrafzadeh, *et al.*

DECEMBER 20, 2022
ANALYTICAL CHEMISTRY

READ 

Get More Suggestions >